TSUNAMI GENERATION DUE TO SUBMARINE VOLCANIC ERUPTIONS WITH PHREATOMAGMATIC EXPLOSION OR CALDERA SUBSIDENCE

Taro Kakinuma[1], Hiroshi Matsumoto[2], Kei Yamashita[3] and Yudai Yanagi[1]

An index of submarine volcanic explosivity concerning tsunami generation has been proposed on the basis of the relationship between phreatomagmatic explosion and resultant initial waveform of tsunamis. In the generation process of tsunamis due to phreatomagmatic explosion, the seawater touches magma of high temperature, after which the water evaporates in an instant with explosive increase of volume. We assume the value of this index specifically to simulate tsunamis caused by submarine volcanic eruption in Kagoshima Bay, where submarine explosion has been observed. Furthermore, tsunamis due to subsidence of a caldera near a volcanic mountain in the same bay are numerically simulated using an initial tsunami profile assumed without discussion about the emission process of magma out of a chamber through submarine volcanic eruption.

Keywords: tsunami generation; submarine volcanic eruption; phreatomagmatic explosion; caldera subsidence

INTRODUCTION

Submarine explosive eruption causes not only a blowout of volcanic products but also phreatomagmatic explosion, resulting in generation of tsunamis (Taniguchi, 1996). In the present study, the mechanism of tsunami generation caused by submarine volcanic eruption is examined considering phreatomagmatic explosion. In the process of submarine phreatomagmatic explosion, the seawater touches magma of high temperature in the neighborhood of seabed, after which the water evaporates in an instant with explosive increase of its volume. A new index of submarine volcanic explosivity concerning tsunami generation is proposed on the basis of the relationship between submarine phreatomagmatic explosion and resultant initial waveform of tsunamis. We assume the value of this index specifically to perform numerical simulation of tsunamis caused by submarine volcanic eruption in Kagoshima Bay, where submarine explosion has been observed (Tsuji, 1997).

On the other hand, in case some magma is emitted out of a chamber owing to volcanic eruption, subsidence of ground occurs leading to appearance of a caldera (Maeno et al., 2006). We also simulate tsunamis due to subsidence of a caldera near a volcanic mountain in the same bay using an initial tsunami profile assumed without discussion about the unclear emission process of magma for the present.

INDEX OF SUBMARINE VOLCANIC EXPLOSIVITY CONCERNING TSUNAMI GENERATION

Cubical Expansion of Water through Evaporation

The mass and density of one mole of liquid water are 18 g and 1 g/cm^3, respectively, such that the one mole of water occupies 18 ml of volume. On the other hand, one mole of vapor assumed to be an ideal gas occupies 22,700 ml of volume at the standard temperature and pressure (STP), where the temperature and pressure are 0℃ and 10^5 Pa, i.e., 1 bar, respectively. Accordingly, when liquid water changes to vapor at STP, the volume of the vapor becomes 22,700/18 $\approx$ 1,261 times as much as that of the liquid water.

If the pressure is p (Pa), then the volume of gas at temperature τ (℃), V, is evaluated by $V = V_0\,(10^5/p)\,(1+\tau/273)$ according to Boyle-Charle's law, where V_0 is the volume of the gas at 0℃.

Consequently, when the liquid water occupying volume $V_{\rm w}$ at STP changes to vapor of volume V at τ (℃) and p (Pa), the volume expansion ratio is

$$\alpha = V / V_{\rm w} = 1{,}261\times10^5\,(1 + \tau / 273) / p. \tag{1}$$

Volume Expansion Ratio of Water through Phreatomagmatic Explosion

Immediately after the magma touches the water, the following equation is satisfied on their interface (Fauske, 1973):

---

[1] Graduate School of Science and Engineering, Kagoshima University, 1-21-40 Korimoto, Kagoshima, Kagoshima 890-0065, Japan
[2] Toko Engineering Consultants, Ltd., 3-3-3 Hakataekihigashi, Hakata-ku, Fukuoka 812-0013, Japan
[3] International Research Institute of Disaster Science, Tohoku University, 468-1 Aramaki Aza-Aoba, Aoba-ku, Miyagi 980-8579, Japan

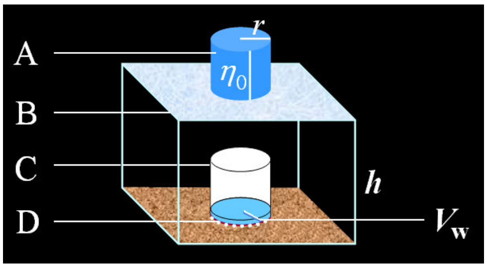

Figure 1. Schematic concept of tsunami generation due to submarine phreatomagmatic explosion (A: the initial tsunami profile, B: still water surface, C: generated vapor, D: crater at the seabed).

$$(\tau_m - \tau_i) / (\tau_i - \tau_w) = (\rho_w c_{pw} k_w / \rho_m c_{pm} k_m)^{1/2}, \tag{2}$$

where τ_i is temperature at the interface between the magma and water; ρ, c_p, and k are density, isopiestic specific heat, and heat transfer coefficient, respectively; the subscripts m and w denote variables of the magma and water, respectively. The general values of these parameters are as follows (Taniguchi, 1996).

[General values of the parameters for magma]
Density $\rho_m = 2{,}400$ kg/m^3
Temperature $\tau_m = 973$ K
Isopiestic specific heat $c_{pm} = 1.2\times10^3$ J/kgK
Heat transfer coefficient $k_m = 1.2$ W/mK

[General values of the parameters for water]
Density $\rho_w = 1{,}000$ kg/m^3
Temperature $\tau_w = 273$ K
Isopiestic specific heat $c_{pw} = 4.2\times10^3$ J/kgK
Heat transfer coefficient $k_w = 0.61$ W/mK

We substitute these values into Eq. (2) to obtain the temperature at the interface, τ_i, as

$$\tau_i = 649 \text{ K} = 376℃. \tag{3}$$

This value is larger than the spontaneous nuclear generation temperature of water, i.e., about 583 K at one atm. Note that the temperature shows an increase of only around 10 K at 2 MPa (Taniguchi, 1996).

Relationship between Volume Expansion Ratio of Seawater near the Seabed and Still Water Depth

The water pressure p at a submarine crater in still water is written by

$$p = \rho_w g h = 9{,}800\, h \text{ (Pa) (unit of length: m)}, \tag{4}$$

where h is still water depth at the location of crater; the gravitational acceleration g equals 9.8 m/s^2. We substitute the value of τ_i shown in Eq. (3) and p given by Eq. (4) into τ and p in Eq. (1), respectively, resulting in

$$\alpha = V / V_w = 30{,}600 / h \text{ (unit of length: m)}, \tag{5}$$

where the water surface displacement is assumed to be much smaller than the still water depth. Equation (5) expresses the relationship between the volume expansion ratio of water over the crater and the still water depth at the location of crater; for instance, $\alpha \approx 10.2$ in case h = 3,000 m, while $\alpha \approx 6.1\times10^2$ in case $h = 50$ m.

Relationship between Submarine Volcanic Explosivity and Initial Tsunami Profile

We assume that a circular crater with radius r appears at the horizontal seabed, with the seawater over the crater then being vaporized to expand vertically in an instant, such that the initial tsunami profile becomes a cylinder as illustrated in Fig. 1, where V_w is original volume of seawater before changing to vapor. Note that the effect of temporal change of bottom configuration on tsunami

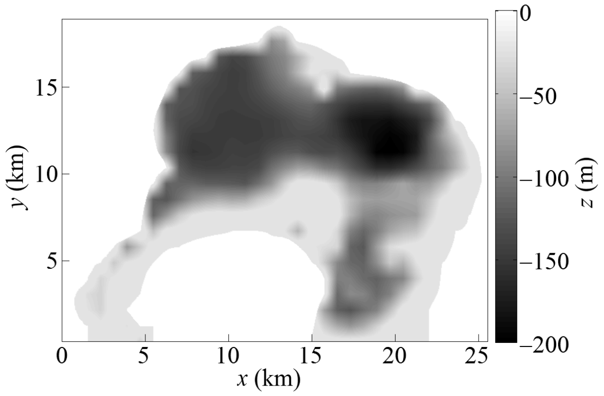

Figure 2. Seabed level in Kagoshima Bay.

generation as discussed by Kakinuma and Akiyama (2007) is neglected for simplicity. The volume of cylinder shown in the figure, V, becomes $\pi r^2 \eta_0$, where η_0 is height of the cylinder, i.e., height of the initial tsunami. Therefore, according to Eq. (5), η_0 is evaluated by

$$V_{\mathrm{w}} = \pi r^2 \eta_0 h / 30{,}600 \approx 1.0 \times 10^{-4} r^2 \eta_0 h \text{ (unit of length: m).} \tag{6}$$

Accordingly, the original volume of seawater, which changes to vapor through phreatomagmatic explosion, V_{w}, is a new index of submarine volcanic explosivity concerning tsunami generation.

NUMERICAL SIMULATION OF TSUNAMIS DUE TO SUBMARINE PHREATOMAGMATIC EXPLOSION IN A BAY

Values of Index of Submarine Volcanic Explosivity Concerning Tsunami Generation

The radius of crater, r, is evaluated by

$$r = 0.97 V_{\mathrm{e}}^{0.36} \text{ (unit of length: m),} \tag{7}$$

where V_{e} is amount of eruption (Sato and Taniguchi, 1997).

In the present paper, the volcanic explosivity index (VEI) devised by Newhall and Self (1982) is assumed to equal three, larger than two in case of the standard explosion, then the amount of eruption, V_{e}, becomes between 10^7 m^3 and 10^8 m^3; the radius r is hence between 321 m and 736 m according to Eq. (7), such that we assume that r equals 700 m.

According to an old document, which reported that the initial tsunami height η_0 was around 9 m owing to the submarine volcanic eruption in Kagoshima Bay, Japan, on Sep. 9, 1780 (Tsuji, 1997), the initial tsunami height η_0 is assumed to equal 9.0 m in the present computation. Thus the value of index of submarine volcanic explosivity concerning tsunami generation, V_{w}, becomes about 2.3×10^4 (unit of length: m) in case the still water depth h equals 50 m around the location of eruption, while $V_{\mathrm{w}} \approx 4.5\times10^4$ (unit of length: m) in case h = 100 m.

Numerical Model and Calculation Conditions

Numerical simulation of tsunamis due to submarine volcanic eruption in Kagoshima Bay is performed using the shallow water version of the nonlinear wave model (Yamashita et al., 2013), where implicit schemes similar to that of Nakayama and Kakinuma (2010) are utilized to solve the fundamental equations. The seabed level in the bay is shown in Fig. 2, where the still water level is described by $z = 0$ m. The shorelines are vertical walls with perfect reflection, while Sommerfeld's radiation condition is applied at the open boundaries. The initial tsunami height η_0 is assumed to be 9.0 m as mentioned above.

Water Surface Displacements

First, water surface displacemetns are obtained through numerical calculation in case the craters are located at Points ① and ③ shown in Fig. 3, as well as the above-mentioned actual case on Sep. 9, 1780, where the crater appeared at Point ② shown in the same figure.

Numerical results of water surface displacements at Points A and B indicated in Fig. 3 are shown in Figs. 4 and 5, respectively. The tsunami height of not only the first wave but also several following

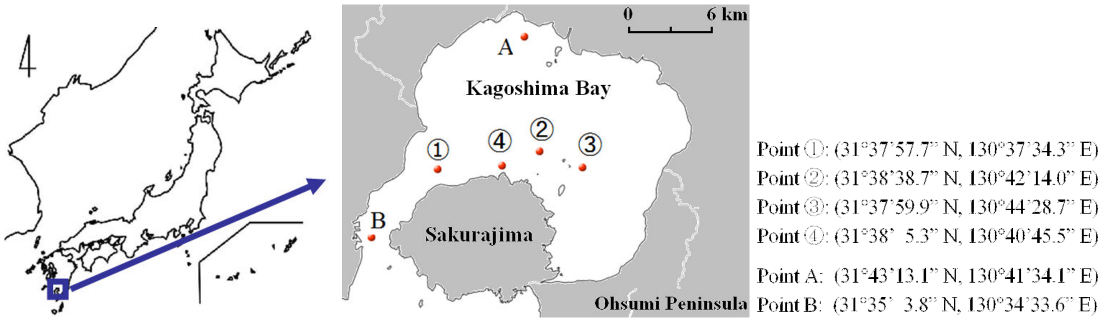

Figure 3. Locations of the points in Kagoshima Bay, Japan. Sakurajima, which was an isolated island, has an active volcano. Point B is located at West Sakurajima Channel.

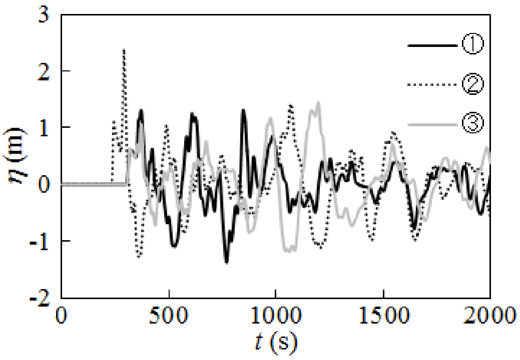

Figure 4. Water surface displacements at Point A shown in Fig. 3. The craters are located at Points ①–③ indicated in the same figure.

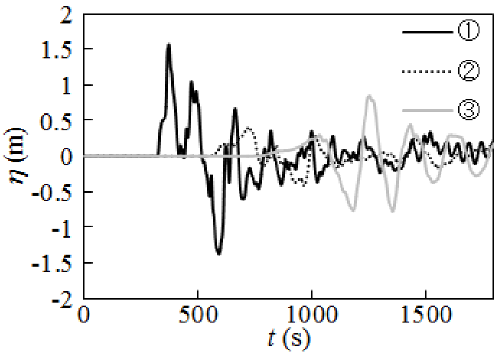

Figure 5. Water surface displacements at Point B shown in Fig. 3. The craters are located at Points ① – ③ indicated in the same figure.

waves is larger than one meter at Point A, where it takes a longer time for the oscillation to attenuate than at Point B because of the multiple reflection at the head of the bay.

Although Point ③ is more distant from Point B than Point ②, the maximum tsunami height at Point B near the urban area in case the crater is located at Point ③ is larger than that in case the crater appears at Point ②, for the energy of wave components which approach the seashore of Sakurajima obliquely or in parallel, resulting in their travel along the shoreline of Sakurajima to the west, is greater in the former than in the latter.

Distribution of the Maximum Water Level

Second, numerical calculaton is carried out in four cases, where the craters are located off the north of Sakurajima, Hayato, Ryugamizu, and Kurokami-cho; the locations of the craters are denoted by white circles in Figs. 6, 7, 8, and 9, respectively. The still water depth at the craters, h, is 100 m in all

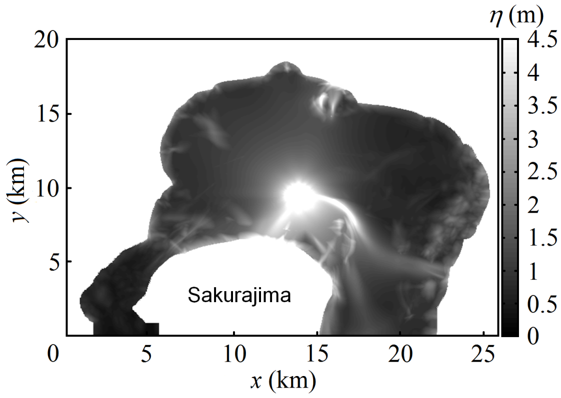

Figure 6. Distribution of the maximum water level while 0 s≦*t*≦2,000 s, where the crater is located off the north of Sakurajima.

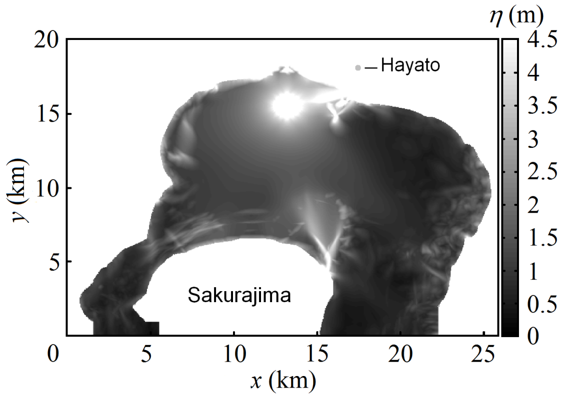

Figure 7. Distribution of the maximum water level while 0 s≦*t*≦2,000 s, where the crater is located off Hayato.

the cases, such that the value of index of submarine volcanic explosivity concerning tsunami generation, V_w, is about 4.5×10^4 (unit of length: m).

Shown in Figs. 6 – 9 are numerical results of distribution of the maximum water level η_{max} while t is from 0 s to 2,000 s. In every case, the maximum water level η_{max} decreases around the spot where (x, y) = (20 km, 14 km), since the still water depth is deeper, i.e., about 200 m at the position.

On the other hand, there are three areas where η_{max} becomes larger without reference to the crater location: as shown in Figs. 6, 7, 8, and 9, near the northern shore of Sakurajima, η_{max} is 5.7 m, 3.2 m, 8.9 m, and 5.4 m, respectively; at the head of the bay off Hayato, η_{max} is 5.4 m, 7.0 m, 3.4 m, and 3.1 m, respectively; near the western shore of Ohsumi Peninsula, η_{max} is 3.6 m, 4.9 m, 4.8 m, and 6.5 m, respectively. In the neighborhood of these three areas, the still water depth suddenly becomes shallower towards the land.

As shown in Fig. 6, the tsunamis generated off the north of Sakurajima travel towards the north after reflecting at the northern shore of Sakurajima, while as Fig. 7 indicates, the tsunamis generated off Hayato propagate towards the south after the reflection at the bay-head shore. In the cases shown in Figs. 8 and 9, however, the tsunamis generated off Ryugamizu and Kurokami-cho propagate towards the east and west, respectively, where the maximum wave height of these components is larger.

NUMERICAL SIMULATION OF TSUNAMIS DUE TO SUBSIDENCE OF A CALDERA IN THE SAME BAY

If some magma is emitted out of a chamber owing to volcanic eruption, subsidence of ground occurs leading to appearance of a caldera (Maeno et al., 2006). The subsidence depth of seabed was reported to be from 1.5 m to 3 m through the generation of caldera in Kagoshima Bay on Nov. 8, 1780 (Tsuji, 1997). We assume that the subsidence depth of seabed equals three meters throughout a caldera,

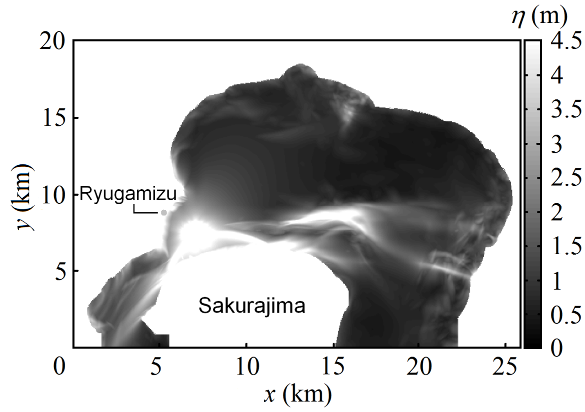

Figure 8. Distribution of the maximum water level while 0 s≦t≦2,000 s, where the crater is located off Ryugamizu.

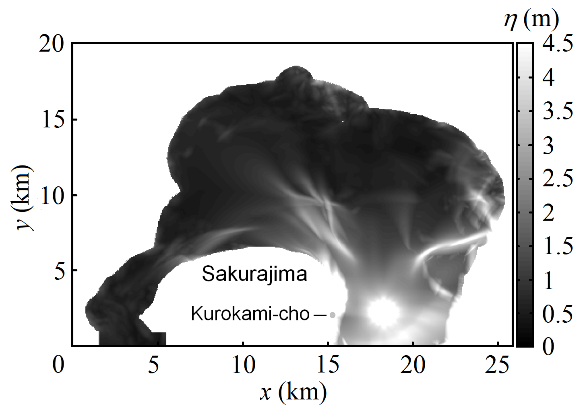

Figure 9. Distribution of the maximum water level while 0 s≦t≦2,000 s, where the crater is located off Kurokami-cho.

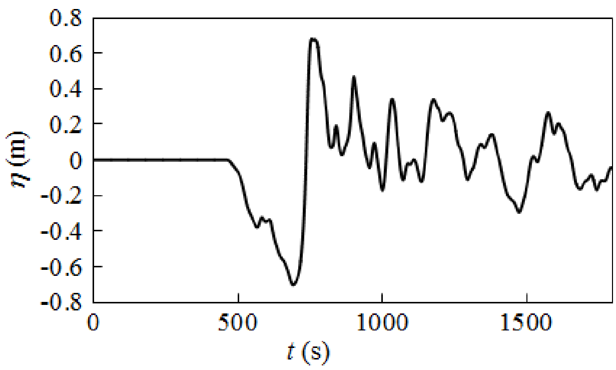

Figure 10. Water surface displacement at Point B shown in Fig. 3. The crater is located at Point ④ indicated in the same figure.

which is a horizontal circle with a center located at Point ④ shown in Fig. 3 and a radius of 1,500 m, without discussion about the unclear emission process of magma for the present.

Shown in Fig. 10 is the calculation result of water surface displacement at Point B indicated in Fig. 3 using the numerical model with computation conditions mentioned above. According to the figure, the water surface displacement of the leading wave is negative at Point B located at West Sakurajima Channel, differently from the results shown in Figs. 4 and 5, where the leading tsunami shows the positive water level owing to the phreatomagmatic explosion.

CONCLUSIONS

The index of submarine volcanic explosivity concerning tsunami generation has been proposed on the basis of the relationship between phreatomagmatic explosion and resultant initial waveform of tsunamis. In the generation process of tsunamis due to phreatomagmatic explosion, the seawater touches magma of high temperature, after which the water evaporates in an instant with explosive increase of volume.

We assumed the value of this index specifically to simulate the tsunamis caused by the submarine volcanic eruption in Kagoshima Bay. It took a longer time for the oscillation to attenuate at the bay head because of the multiple reflection. The maximum water level was larger without reference to the location of crater near the northern shore of Sakurajima, at the head of the bay off Hayato, and near the western shore of Ohsumi Peninsula, where the still water depth suddenly became shallower towards the coast. In case the tsunamis approached the seashore of Sakurajima obliquely or in parallel, they traveled along the shoreline: the tsunamis generated off Ryugamizu and Kurokami-cho propagated along the shoreline of Sakurajima towards the east and west, respectively, where the maximum wave height of these components was larger.

The tsunamis due to the subsidence of caldera in the same bay were also simulated numerically in case magma was supposed to be emitted out of its chamber owing to submarine volcanic eruption. The water surface displacement of the leading wave was negative at West Sakurajima Channel, differently from that of the tsunamis due to the phreatomagmatic explosion.

Future work is required to investigate the shape of water vapor generated through submarine phreatomagmatic explosion, as well as the emission process of magma out of its chamber to cause subsidence of a caldera.

REFERENCES

Fauske, H. K. 1973. On the mechanism of uranium dioxide-sodium explosive interactions, *Nuclear Science and Engineering*, 51, 95-101.

Kakinuma, T. and M. Akiyama. 2007. Numerical analysis of tsunami generation due to seabed deformation, *Proceedings of 30th International Conference on Coastal Engineering*, ASCE, 1490-1502.

Maeno, F., F. Imamura and H. Taniguchi. 2006. Numerical simulation of tsunamis generated by caldera collapse during the 7.3 ka Kikai eruption, Kyushu, Japan, *Earth Planets Space*, 58, 1013-1024.

Nakayama, K. and T. Kakinuma. 2010. Internal waves in a two-layer system using fully nonlinear internal-wave equations, *International Journal for Numerical Methods in Fluids*, 62, 574-590.

Newhall, C. G. and S. Self. 1982. The volcanic explosivity index (VEI): An estimate of explosive magnitude for historical volcanism, *Journal of Geophysical Research*, 87, C2, 1231-1238.

Sato, H. and H. Taniguchi. 1997. Relationship between crater size and ejecta volume of recent magmatic and phreato-magmatic eruptions: Implications for energy partitioning, *Geophysical Research Letters*, 24, 205-208.

Taniguchi, H. 1996. Mechanism of a phreatomagmatic explosion due to the interaction between hot rhyolitic lava flow and external water, *Memoirs of the Geological Society of Japan*, 46, 149-162 (in Japanese with an English abstract).

Tsuji, Y. 1997. Volcanic activity and tsunami generation, *Volcano and Magma* (Ed. by Kaneoka, I. and Y. Ide), The University of Tokyo Press, 194-206 (in Japanese).

Yamashita, K., T. Kakinuma and K. Nakayama. 2013. Shoaling of nonlinear internal waves on a uniformly sloping beach, *Proceedings of 33rd International Conference on Coastal Engineering*, ASCE, waves.72, 13 pages.